# Electrooptical Effects in Silicon

RICHARD A. SOREF, SENIOR MEMBER, IEEE, AND BRIAN R. BENNETT

*Abstract*—A numerical Kramers–Kronig analysis is used to predict the refractive-index perturbations produced in crystalline silicon by applied electric fields or by charge carriers. Results are obtained over the 1.0–2.0 $\mu$m optical wavelength range. The analysis makes use of experimental electroabsorption spectra and impurity-doping spectra taken from the literature. For electrorefraction at the indirect gap, we find $\Delta n = 1.3 \times 10^5$ at $\lambda = 1.07$ $\mu$m when $E = 10^5$ V/cm, while the Kerr effect gives $\Delta n = 10^{-6}$ at that field strength. The charge-carrier effects are larger, and a depletion or injection of $10^{18}$ carriers/cm$^3$ produces an index change of $\pm 1.5 \times 10^{-3}$ at $\lambda = 1.3$ $\mu$m.

## I. INTRODUCTION

GUIDED-WAVE components for operation at the 1.3 and 1.6 $\mu$m fiber-optic wavelengths were constructed recently in crystalline silicon [1]–[3]. Passive components such as channel waveguides and power splitters were demonstrated in the initial work, but the next phase of research will deal with active components such as electrooptical switches and modulators controlled by voltage or by current. This paper estimates the size of voltage effects and current effects that may be expected in such devices. The Pockels effect is absent in bulk, unstrained silicon; thus, other electrooptic effects are considered here.

The active crystalline–silicon (c-Si) devices can be loss modulators or phase modulators. In this paper, we shall emphasize devices that modify the phase of a guided optical wave without modifying the wave amplitude. In other words, we are investigating low-loss phase-shifting mechanisms based upon a controlled change in the refractive index of the waveguide medium.

The goal of this paper is to calculate the refractive-index change ($\Delta n$) of c-Si produced by an applied electric field ($E$) or by a change in the concentration of charge carriers ($\Delta N$). Changes in the optical absorption coefficient of the material ($\Delta \alpha$) at the wavelength of interest will be examined to verify that low-loss propagation is achieved. For room-temperature material, results are given here over the optical wavelength range from 1.0 to 2.0 $\mu$m.

## II. THEORY

The complex refractive index may be written as $n + ik$ where the real part $n$ is the conventional index and the imaginary part $k$ is the optical extinction coefficient. $k$ is related to $\alpha$, the linear absorption coefficient, by the relation $k = \alpha\lambda/4\pi$ where $\lambda$ is the optical wavelength. It is well known that $n$ and $k$ are related by the Kramers–Kronig dispersion relations. The same relations hold for $\Delta n$ and $\Delta k$ as discussed below. It has been known for many years that the optical absorption spectrum of silicon is modified by external electric fields (the Franz–Keldysh effect) or by changes in the material's charge-carrier density. If we start with an experimental knowledge of the modified spectrum $\Delta \alpha(\omega, E)$ or $\Delta \alpha(\omega, \Delta N)$, then we can compute the change in the index $\Delta n$.

The Kramers–Kronig coupling between $\Delta n$ and $\Delta \alpha$ has been specified in several textbooks and journal articles, as follows:

$$\Delta n(\omega) = (c/\pi) P \int_0^\infty \frac{\Delta\alpha(\omega')\, d\omega'}{\omega'^2 - \omega^2} \qquad (1)$$

where $\hbar\omega$ is the photon energy. Absorption may be modified by an altered free-carrier concentration:

$$\Delta\alpha(\omega, \Delta N) = \alpha(\omega, \Delta N) - \alpha(\omega, 0)$$

or $\alpha$ may be changed by an applied electric field:

$$\Delta\alpha(\omega, E) = \alpha(\omega, E) - \alpha(\omega, 0).$$

The units of $\alpha$ are typically cm$^{-1}$. The photon energy is expressed in electron-volts, so it is convenient to work with the normalized photon energy "$V$" where $V = \hbar\omega/e$. Recognizing that the quantity $hc/2\pi^2 e = 6.3 \times 10^{-6}$ cm $\cdot$ V, we can rewrite (1) as

$$\Delta n(V) = 6.3 \times 10^{-6} \text{ cm} \cdot \text{V } P \int_0^\infty \frac{\Delta\alpha(V')\, dV'}{V'^2 - V^2}. \qquad (2)$$

## III. ELECTRIC-FIELD EFFECTS

The Franz–Keldysh effect, which alters the $\alpha$ spectrum of c-Si, is field-induced tunneling between valence and conduction band states. In recent years, the generic term "electroabsorption" has been adopted for $\Delta \alpha$ versus $E$ effects. The companion effect, electrorefraction, is investigated here. It is assumed that the starting material has high resistivity or is undoped so that ohmic losses are minimized.

In this paper, we shall consider electroabsorption at the indirect gap of c-Si ($E_g = 1.12$ eV). The electroabsorption spectrum at the indirect edge has been measured in detail by Wendland and Chester [4]. Their experimental data are given in Fig. 1. We digitized the $\Delta \alpha$ curves in Fig. 1 and entered the data in a Hewlett-Packard model 9000-300 computer that was used for the dispersion cal-
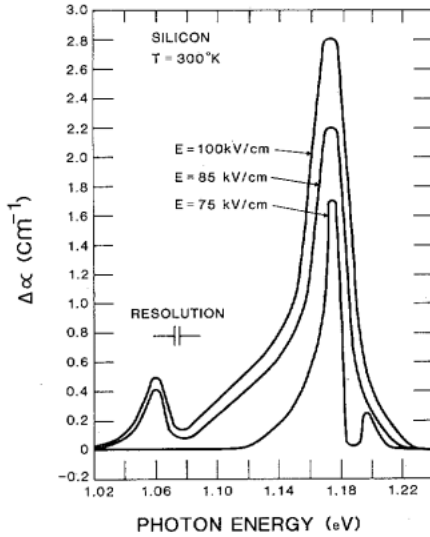
Fig. 1. Electroabsorption data from Wendland and Chester [4, Fig. 3] at the indirect gap of c–Si.
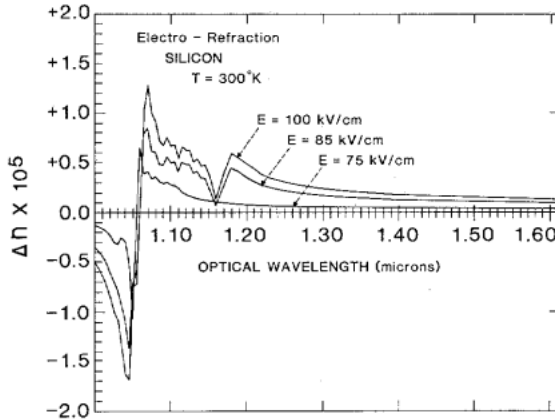


Fig. 2. Electrorefraction versus $\lambda$ in c–Si, determined from Fig. 1.



Fig. 3. Field dependence of electrorefraction at two wavelengths, as determined from Fig. 2. The dashed lines are extrapolations.

culation. Numerical integration per (2) was carried out using the trapezoid rule, with an abscissa interval of 1 meV. A computer routine was used to interpolate values of the $\Delta\alpha$ curve between entered points.

The quantity $\Delta n(\hbar\omega)$ was calculated over the range from $\hbar\omega = 0.77$ to $1.23$ eV. This range includes a transparent region and a 0.11 eV excursion above the nominal gap. Then, $\Delta n$ was expressed as a function of optical wavelength from 1.00 to 1.60 $\mu$m. These electrorefraction results are shown in Fig. 2. It is found that $\Delta n$ is positive for $\lambda > 1.05$ $\mu$m, and that $\Delta n$ is a strong function of wavelength. Starting at 1.3 $\mu$m, as $\lambda$ is decreased towards the gap wavelength, $\Delta n$ rises rapidly and reaches a maximum at 1.07 $\mu$m, a wavelength slightly below the nominal $\lambda_g$. Then, as $\lambda$ decreases further, $\Delta n$ decreases and becomes negative. We find at 1.07 $\mu$m that $\Delta n = +1.3 \times 10^{-5}$ when $E = 10^5$ V/cm.

The change in index as a function of applied $E$ field is plotted in Fig. 3 at the optimum 1.07 $\mu$m wavelength and at the nearby 1.09 $\mu$m wavelength. The rate of increase $\Delta n/\Delta E$ is found to be slightly faster than $E^2$, and at 1.07
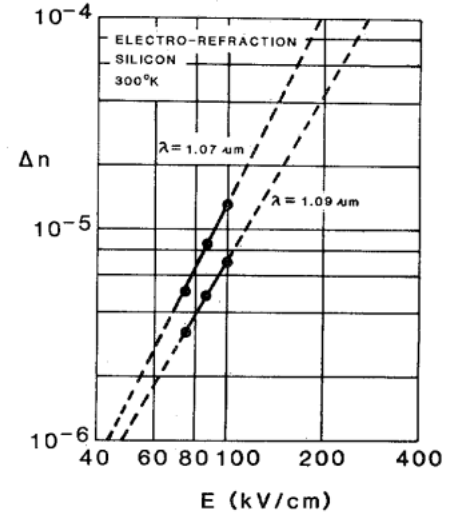
$\mu$m the extrapolated value of $\Delta n$ reaches $10^{-4}$ at $E = 2 \times 10^5$ V/cm. The dielectric breakdown strength of silicon is $4 \times 10^5$ V/cm at $N_i = 10^{15}$ cm$^{-3}$ (Fig. 2-13 of Sze [5]).

Electroabsorption is present at the direct gap of silicon ($E_{g'} = 3.4$ eV); however, transmission measurements of electroabsorption near 3.4 eV are precluded by the high zero-field absorption at these photon energies. The 3.4 eV region can be accessed with electroreflectance measurements [6]. The refractive-index perturbations at $\lambda = 1.07$ $\mu$m caused by direct-gap electroabsorption are expected to be smaller than the indirect-gap $\Delta n$'s and are related to the Kerr effect discussed below.

Judging from the Si electroabsorption results of Gutkin et al. [7], [8], we expect a polarization dependence of electrorefraction. We predict that electrorefraction will be $2\times$ stronger for $\vec{E}_{\text{opt}} \parallel \vec{E}_{\text{appl}}$ than for $\vec{E}_{\text{opt}} \perp \vec{E}_{\text{appl}}$ where $\vec{E}_{\text{opt}}$ is the linearly polarized optical field and $\vec{E}_{\text{appl}}$ is the applied field. (It is assumed that light propagates at 90° to $\vec{E}_{\text{appl}}$.) These predictions hold for $\vec{E}_{\text{appl}} \parallel \langle 100 \rangle$ or for $\vec{E}_{\text{appl}} \parallel \langle 111 \rangle$.

Another "pure field effect," the Kerr effect, is present in Si. We have estimated the strength of the Kerr effect in c–Si using the anharmonic oscillator model of Moss et al. [9]. We used (9.33) in their book and made the approximation $\omega \ll \omega_0$, which gives the result

$$\Delta n = -3e^2(n^2 - 1)E^2/2nM^2\omega_0^4 x^2 \qquad (3)$$

a perturbation that is independent of optical wavelength in this model. Here, $e$ is the electronic charge, $n$ is the unperturbed refractive index, $M$ is the effective mass, $\omega_0$ is the oscillator resonance frequency, and $x$ is the average oscillator displacement. Using the values in Moss' discussion ($n = 3.50$ at $\lambda = 1.3$ $\mu$m, $M = $ the electron mass, $\omega_0 = 2\pi \times 10^{15}$ rad/s, and $x = 10^{-9}$ m), we find from (3) the result shown in Fig. 4, a plot of $\Delta n$ versus applied $E$ field. The predicted $\Delta n$ reaches $10^{-4}$ at $E = 10^6$ V/cm.
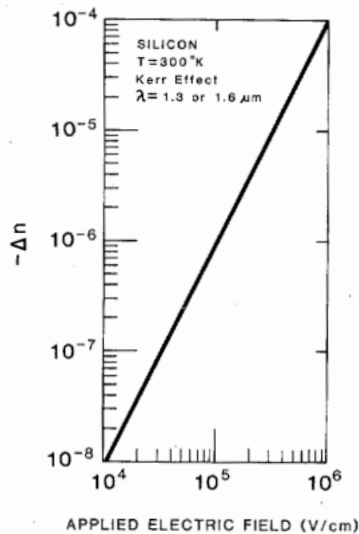
Fig. 4. Kerr effect in c–Si versus $E$ as determined from anharmonic oscillator model.



Fig. 5. Optical absorption spectra of c–Si showing the influence of various concentrations of free electrons.



Fig. 6. Absorption of c–Si at $\lambda = 87 \ \mu m$ as a function of free-carrier concentration.

There is uncertainty about the sign of the Kerr effect. The anharmonic oscillator model predicts a negative $\Delta n$, while a four-wave mixing experiment [10] suggests that $\Delta n$ is positive.

## IV. Charge-Carrier Effects

The optical properties of silicon are strongly affected by injection of charge carriers into an undoped sample ($\Delta N$) or by the removal of free carriers from a doped sample ($-\Delta N$). However, we are not aware of any experimental results in the Si literature on spectral changes via injection/depletion. There are, on the other hand, numerous literature references to the effects of impurity doping on Si optical properties. Optically, it does not make much difference whether carriers come from impurity ionization or from injection. Thus, an equivalence is assumed here. We draw upon experimental results that show how the $\alpha$ spectrum is changed by a density $N_i$ of impurity atoms in the crystal. The $\Delta n$ calculated from that spectrum is assumed to be the $\Delta n$ that arises from $\Delta N$.

Three carrier effects are important: 1) traditional free-carrier absorption, 2) Burstein–Moss bandfilling that shifts the $\alpha$ spectrum to shorter wavelengths, and 3) Coulombic interaction of carriers with impurities, an effect that shifts the spectrum to longer wavelengths. These act simultaneously. What is actually observed is an $\alpha$ redshift; thus, Coulombic effects are stronger than bandfilling in c–Si (see [11] and [12]).

For impurity concentrations in the $10^{18}$–$10^{20}$ cm$^{-3}$ range, Schmid [11] has given detailed absorption spectra for $n$-type and $p$-type silicon in both the transparent ($\hbar\omega < E_g$) and opaque ($\hbar\omega > E_g$) regions covering 0.6 eV $< \hbar\omega < 1.5$ eV. His data are the basis for our Kramers–Kronig inversion. Spitzer and Fan [13] also present data for $n$-type material over a wide infrared range from 0.025 to 1.1 eV. They find a weak absorption band from 0.25 to 0.82 eV. Using the above data, Fig. 5 is a composite
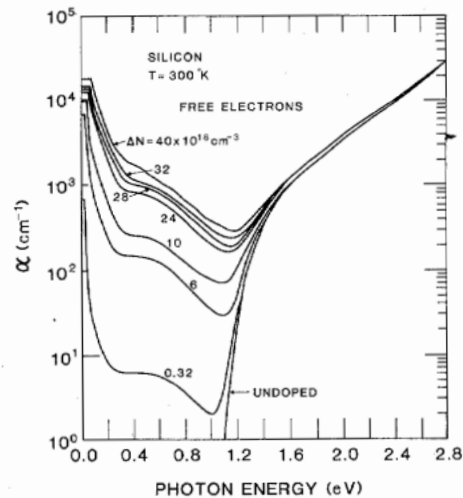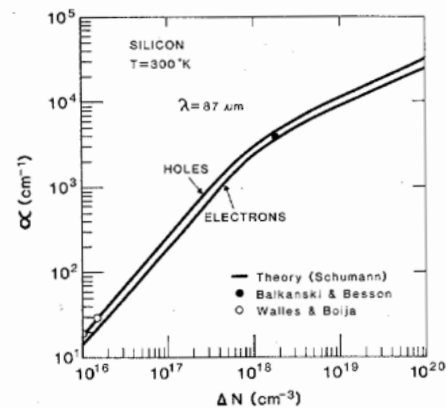
drawing of optical absorption versus $\hbar\omega$ for various concentrations $\Delta N$ of free electrons. For the undoped material in Fig. 5, we used the data of Dash and Newman [14], Spitzer and Fan [13], and Schmid [11]. Over the 0.25–0.82 eV range, we extrapolated Schmid's doping curves to follow the spectral shape of Spitzer and Fan's data.

In $n$-type Si, for wavelengths longer than the 5 $\mu m$ absorption band edge, the experimental results of [13] show that free-carrier absorption follows a $\lambda^2$ law out to $\lambda = 50 \ \mu m$ for samples with $8 \times 10^{16}$ cm$^{-3}$ doping. In addition, Balkanski and Besson [15] observe that $\alpha$ in $n$-type samples saturates or "levels off" over the 50–87 $\mu m$ range. Randal and Rawcliffe [16] find that the $\alpha(\lambda)$ spectrum is flat from $\lambda = 100$ to 500 $\mu m$. For these reasons, we conclude that the Fig. 5 curves should include a leveling off of $\alpha$ in the far infrared, as well as the $\alpha \sim \lambda^2$ middle-infrared behavior mentioned above.

Schumann *et al.* [17, Fig. 142] have presented a curve of $\alpha$ versus $\Delta N$ in $n$-type Si at the 87 $\mu m$ wavelength, a curve reproduced here as Fig. 6. On this curve, we have plotted the experimental result of [15]. Also plotted in Fig. 6 is a theoretical curve for $p$-type Si, a curve drawn
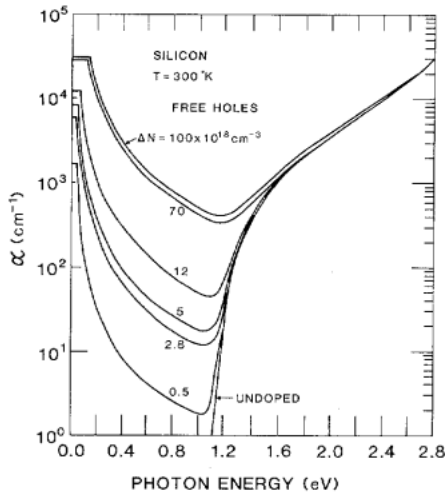
Fig. 7. Optical absorption spectra of c-Si showing the influence of various concentrations of free holes.



Fig. 8. Refractive-index perturbation of c–Si (versus $\lambda$) produced by various concentrations of free electrons.



Fig. 9. Refractive-index perturbation of c–Si (versus $\lambda$) produced by various concentrations of free holes.

through the two experimental data points of Walles and Boija [18], [19]. The curves in Fig. 6 show the absorption plateaus that are reached by $\alpha(\lambda)$ in the far infrared. This information is used in Fig. 5 where the $\alpha(\omega)$ curves for the various $\Delta N$'s were flattened (as shown) at the values taken from Fig. 6. The saturation of $\alpha$ at low frequencies is also consistent with the reflectivity measurements of Schumann and Phillips [20]. Above each plateau, an $\omega^{-2}$ extrapolation is used in Fig. 5. In the higher frequency portion of Fig. 5, ($\hbar\omega > 1.2$ eV), we assumed that the various curves merged smoothly into the undoped curve as shown. The merger is complete above 2.8 eV. In Fig. 5, the range of integration used for the Kramers–Kronig inversion was 0.001–2.8 eV.

A composite drawing for $p$-type Si is shown in Fig. 7. This figure presents experimental $\alpha$ versus $\hbar\omega$ data for various concentrations $\Delta N$ of free holes. Unlike $n$-type material, the $p$-type Si does not show the near-infrared absorption band, and several investigators have found that free-hole absorption follows a $\lambda^2$ law reasonably well over the near and middle infrared. Hence, an $\omega^{-2}$ extrapolation of Schmid's data is used in Fig. 7. The prior three literature sources are used for the undoped sample spectrum. As in Fig. 5, we again take into account the leveling off of $\alpha$ in the far infrared. The saturation values of $\alpha(\lambda)$ at 87 $\mu$m for $p$-type Si are found in Fig. 6 for the different $\Delta N$ values of Fig. 7, and these plateaus are used in Fig. 7 near 0.1 eV as shown. The merging of curves at $\hbar\omega > 1.2$ eV in Fig. 7 is similar to that in Fig. 5. As in Fig. 5, the range of integration in Fig. 7 for (2) was 0.001–2.8 eV.

With the aid of $x$-$y$ lines drawn on Figs. 5 and 7, the ($\alpha$, $\omega$) data were digitized and entered into the computer, and the absorption spectrum of pure material was subtracted point by point from each of the quantized $\alpha(\Delta N)$ curves to give a set of $\Delta\alpha$ values that were inserted into the numerator of (2). With our trapezoid-rule program, we calculated the integral (2) over the range $V = 0.001$–2.8 V, and we took $N_i = \Delta N$. This produced the result
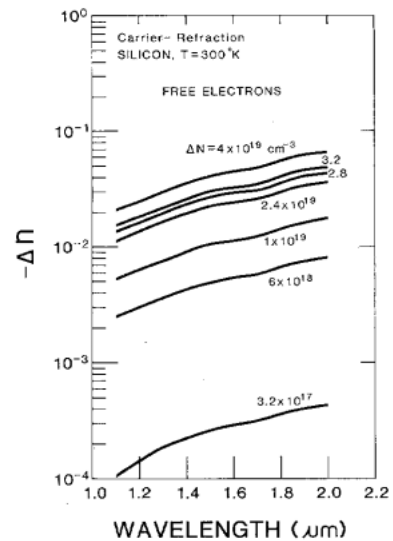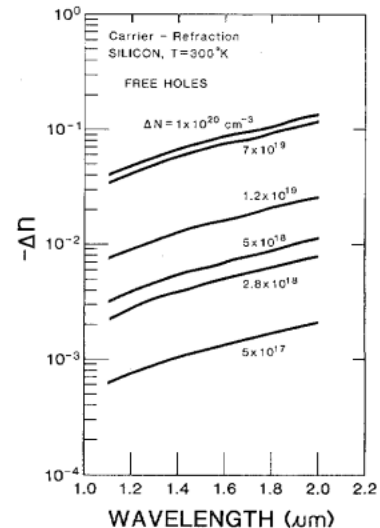
shown in Fig. 8 for free electrons and the result of Fig. 9 for free holes. Figs. 8 and 9 are plots of $\Delta n$ as a function of wavelength from 1.0 to 2.0 $\mu$m with $\Delta N$ as a parameter. The increase of $\Delta n$ with $\lambda$ is approximately quadratic. Next, we used the results of Figs. 8 and 9 to determine the carrier-concentration dependence of $\Delta n$ at the fiber-optic wavelengths: $\lambda = 1.3$ or $1.55$ $\mu$m. Those results are shown in Figs. 10 and 11. The curves presented in Figs. 10 and 11 are least squares fit to the data points obtained from Figs. 8 and 9. In Fig. 10 ($\lambda = 1.3$ $\mu$m), the free-hole data are fitted with a line of slope $+0.805$, while the free-electron data are fitted with a $+1.05$ slope line. In Fig. 14 ($\lambda = 1.55$ $\mu$m), the fitted slopes are $+0.818$(holes) and $+1.04$(electrons).

It is interesting to compare the predictions of a simple free-carrier or Drude model of c–Si to our $\Delta n$ results and to experimental $\Delta\alpha$ data. The well-known formulas for
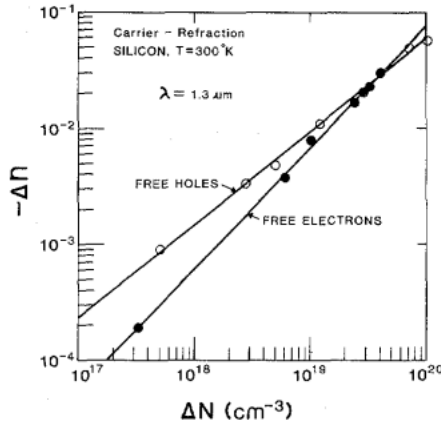
Fig. 10. Carrier refraction in c–Si at $\lambda = 1.3$ $\mu$m as a function of free-carrier concentration ($\Delta n$ determined from Figs. 8 and 9).
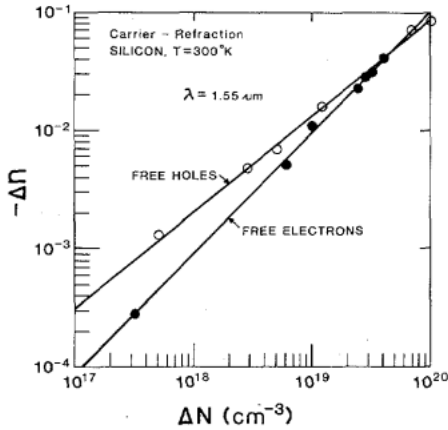


Fig. 12. Absorption in c–Si at $\lambda = 1.3$ $\mu$m as a function of free-electron concentration.



Fig. 11. Carrier refraction in c–Si at $\lambda = 1.55$ $\mu$m as a function of free-carrier concentration ($\Delta n$ determined from Figs. 8 and 9).



Fig. 13. Absorption in c–Si at $\lambda = 1.3$ $\mu$m as a function of free-hole concentration.



Fig. 14. Absorption in c–Si at $\lambda = 1.55$ $\mu$m as a function of free-electron concentration.

refraction and absorption due to free electrons and free holes are as follows:

$$\Delta n = -(e^2\lambda^2/8\pi^2c^2\epsilon_0 n)\,[\Delta N_e/m_{ce}^* + \Delta N_h/m_{ch}^*] \quad (4)$$

$$\Delta\alpha = (e^3\lambda^2/4\pi^2c^3\epsilon_0 n)\,[\Delta N_e/m_{ce}^{*2}\mu_e + \Delta N_h/m_{ch}^{*2}\mu_h] \quad (5)$$

where $e$ is the electronic charge, $\epsilon_0$ is the permittivity of free space, $n$ is the refractive index of unperturbed c–Si, $m_{ce}^*$ is the conductivity effective mass of electrons, $m_{ch}^*$ is the conductivity effective mass of holes, $\mu_e$ is the electron mobility, and $\mu_h$ is the hole mobility.

We shall consider first the added loss introduced by free electrons or free holes. Theoretical curves from (5) are plotted together with the experimental absorption values taken from Schmid [11] and from Spitzer and Fan [13]. Curves for electrons and holes at the 1.3 and 1.55 $\mu$m wavelengths are given as a function of "injected" carrier concentration in Figs. 12–15. The theoretical curves in Figs. 12–15 were obtained by substituting the values $m_{ce}^* = 0.26\,m_0$ and $m_{ch}^* = 0.39\,m_0$ into (5). The mobility values used in (5) were taken from Fig. 2.3.1 of Wolf [21]. An examination of Figs. 12–15 reveals that the $\Delta\alpha$'s pre-
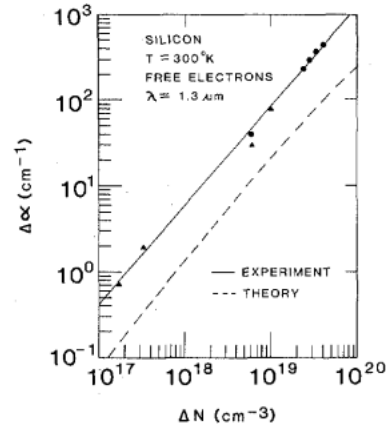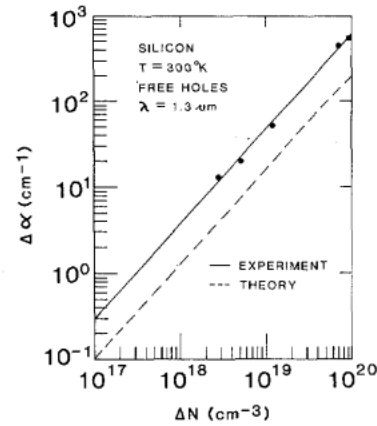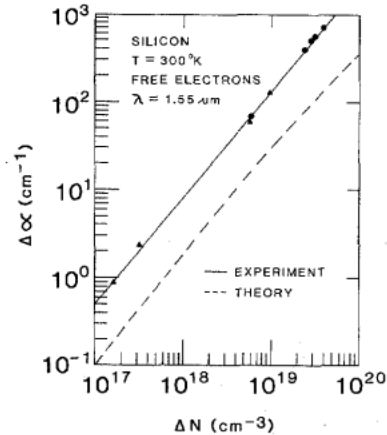
dicted from simple theory are approximately 0.5 of the actual values for holes, and are approximately 0.25 of the experimental values for electrons.

We consider now the $\Delta n$ results of Figs. 8–11. Generally, we found that free holes are more effective in perturbing the index than free electrons, especially at $\Delta N =$
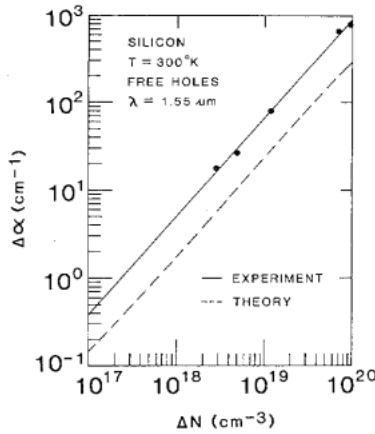
Fig. 15. Absorption in c–Si at $\lambda = 1.55$ $\mu$m as a function of free-hole concentration.



Fig. 16. Length required for 180° phase shift and optical throughput loss as a function of carrier concentration.

$10^{17}$ cm$^{-3}$ where $\Delta n$(holes) $= 3.3$ $\Delta n$(electrons). This result differs from the Drude theory result obtained from (4) above where $\Delta n$(holes) $= 0.66$ $\Delta n$(electrons) over the entire $\Delta N$ range (see [3, Fig. 2]). For electrons, the results in Figs. 8–11 are in good agreement with the prediction of (4) [3, Fig. 2] but for holes, the $(\Delta N)^{0.8}$ dependence of Figs. 8–11 differs from the $\Delta n \sim \Delta N$ prediction of simple theory.

## V. Discussion

Electrorefraction and carrier refraction have been analyzed here. Generally speaking, carrier refraction is the larger effect. It should be noted that the refractive index will increase when carriers are depleted from doped material [22]; conversely, the index will decrease when carriers are injected. The modulation is polarization independent. In the injection case, the switch-off time will probably be limited by minority carrier lifetime (ns to $\mu$s). However, the depletion mode is expected to offer much faster response times, possibly in the picosecond range, because of carrier sweep out. (Depletion experiments in III–V materials are discussed in [23] and [24].) The inherent on/off response times of electrorefraction are subpicosecond. The response in practice is limited by the $RC$ time constants of the electrooptic device.

We want to obtain practical design rules for guided-wave modulators and $2 \times 2$ switches that use electrooptic phase modulation (PM) without significant amplitude modulation (AM). However, it will be impossible to reach the PM-without-AM condition because a finite $\Delta n$ is always correlated with a finite $\Delta \alpha$. Nevertheless, we believe that a meaningful tradeoff can be made between phase shift and loss, so that complete $2 \times 2$ switching can be attained with less than 1 dB of excess optical loss. The tradeoffs are illustrated in Fig. 16 where we have plotted the interaction length required for $\pi$ rad phase shift and the optical throughput loss produced by this length. Both quantities are plotted as a function of carrier concentration. In Fig. 16, we focused on the case of free-hole depletion/injection at $\lambda = 1.3$ $\mu$m. The length $L_\pi$ is given by $\lambda/2\De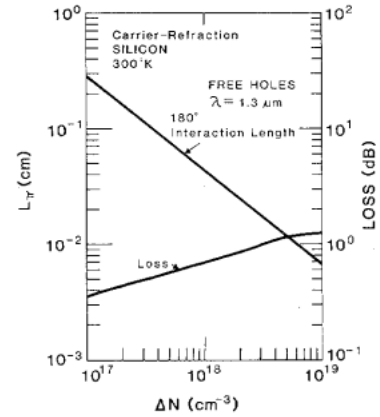lta n$, and $\Delta n$ is taken from Fig. 10. The loss in decibels is given by 10 log $\{\exp [-(\alpha_0 + \Delta\alpha)L_\pi]\}$ and $\Delta\alpha$ is taken from the Fig. 13 experimental values. Submillimeter lengths with $< 1$ dB of loss are seen in Fig. 16. To get an idea of the optical loss associated with electrorefraction, we note from Fig. 1 that $\Delta\alpha(1.07$ $\mu$m) $= 1.9$ cm$^{-1}$ and $\Delta\alpha(1.09$ $\mu$m) $= 0.8$ cm$^{-1}$ when $E = 10^5$ V/cm, while the initial $E = 0$ loss from Fig. 5 (undoped Si) is $\alpha_0(1.07$ $\mu$m) $= 10$ cm$^{-1}$ and $\alpha_0(1.09$ $\mu$m) $= 5$ cm$^{-1}$.

## VI. Summary

We have performed numerical integration of electroabsorption spectra and impurity-doping spectra (taken from the c–Si literature) to estimate the refractive-index perturbations produced by applied fields or by injected/depleted carriers. At $\lambda = 1.07$ $\mu$m, an electrorefraction of $\Delta n = +1.3 \times 10^{-5}$ was found for $E = 10^5$ V/cm. This was due to indirect-gap electroabsorption. Carrier refraction over the $10^{17}$–$10^{20}$ carrier/cm$^3$ range was determined. For a depletion of $10^{18}$ free holes per cm$^3$, we found $\Delta n = +1.5 \times 10^{-3}$ at $\lambda = 1.3$ $\mu$m and $\Delta n = +2.1 \times 10^{-3}$ at $\lambda = 1.55$ $\mu$m with $\Delta n \sim (\Delta N)^{0.8}$ for holes and $\Delta n \sim (\Delta N)^{1.05}$ for electrons.

## References

[1] R. A. Soref and J. P. Lorenzo, "Single-crystal silicon—A new material for 1.3 and 1.6 $\mu$m integrated-optical components," *Electron. Lett.*, vol. 21, pp. 953–955, Oct. 10, 1985.

[2] ——, "Epitaxial silicon guided-wave optical components for $\lambda = 1.3$ $\mu$m," in *Dig. Papers, 1986 Integrated and Guided-Wave Opt. Conf.*, Atlanta, GA, Feb. 26, 1986, paper WDD5, pp. 18–19.

[3] ——, "All-silicon active and passive guided-wave components for $\lambda = 1.3$ and 1.6 $\mu$m," *IEEE J. Quantum Electron.*, vol. QE-22, pp. 873–879, June 1986.

[4] P. H. Wendland and M. Chester, "Electric field effects on indirect optical transitions in silicon," *Phys. Rev.*, vol. 140, no. 4A, p. 1384, 1965.

[5] S. M. Sze, *Physics of Semiconductor Devices*, 2nd ed.   New York: Wiley, 1981.

[6] B. O. Seraphin, "Optical field effect in silicon," *Phys. Rev.*, vol. 140, no. 5A, pp. A1716–1725, 1965.

[7] A. A. Gutkin, D. N. Nasledov, and F. E. Faradzhev, "Influence of the orientation of the electric field on the polarization dependence of electroabsorption in silicon," *Sov. Phys. Semicond.*, vol. 8, p. 781, Dec. 1974.

[8] A. A. Gutkin and F. E. Faradzhev, "Influence of the polarization of light on the electroabsorption in silicon," *Sov. Phys. Semicond.*, vol. 6, p. 1524, Mar. 1973.

[9] T. S. Moss, G. J. Burrell, and B. Ellis, *Semiconductor Opto-Electronics.* London: Butterworths, 1973.

[10] J. J. Wynne and G. D. Boyd, "Study of optical difference mixing in Ge and Si using a $CO_2$ gas laser," *Appl. Phys. Lett.*, vol. 12, pp. 191–192, 1968.

[11] P. E. Schmid, "Optical absorption in heavily doped silicon," *Phys. Rev. B*, vol. 23, p. 5531, May 15, 1981.

[12] A. A. Volfson and V. K. Subashiev, "Fundamental absorption edge of silicon heavily doped with donor or acceptor impurities," *Sov. Phys. Semicond.*, vol. 1, no. 3, pp. 327–332, Sept. 1967.

[13] W. Spitzer and H. Y. Fan, "Infrared absorption in n-type silicon," *Phys. Rev.*, vol. 108, p. 268, 1957.

[14] W. C. Dash and R. Newman, "Intrinsic optical absorption in single-crystal germanium and silicon," *Phys. Rev.*, vol. 99, pp. 1151–1155, 1955.

[15] M. Balkanski and J. M. Besson, "Optical properties of degenerate silicon," Tech. Note 2, Contract AF61(052)-789, Defense Tech. Inform. Cen., AD 619581, 1965.

[16] C. M. Randall and R. D. Rawcliffe, "Refractive indices of germanium, silicon, and fused quartz in the far infrared," *Appl. Opt.*, vol. 6, p. 1889, 1967.

[17] P. A. Schumann Jr., W. A. Keenan, A. H. Tong, H. H. Gegenwarth, and C. P. Schneider, "Optical constants of silicon in the wavelength range 2.5 to 40 $\mu$m," IBM Tech. Rep. TR-22.1008, East Fishkill, NY, May 20, 1970.

[18] S. Walles, "Transmission of silicon between 40 and 100 $\mu$m," *Arkiv Fysik*, vol. 25, no. 4, p. 33, 1963–1964.

[19] S. Walles and S. Boija, "Transmittance of doped silicon between 40 and 100 $\mu$m," *J. Opt. Soc. Amer.*, vol. 54, pp. 133–134, Jan. 1964.

[20] P. A. Schumann and R. P. Phillips, "Comparison of classical approximation to free carrier absorption in semiconductors," *Solid State Electron.*, vol. 10, p. 943, 1967.

[21] H. F. Wolf, *Silicon Semiconductor Data.* London: Pergamon, 1969.

[22] Silicon channel waveguides with lateral dimensions in the range from 0.2 to 0.6 $\mu$m will support a single propagating mode at $\lambda = 1.3$ $\mu$m. In submicron structures of this kind, depletion of high carrier densities can be accomplished with practical voltages.

[23] X. S. Wu, A. Alping, A. Vawter, and L. A. Coldren, "Miniature optical waveguide modulator in AlGaAs/GaAs using carrier depletion," *Electron. Lett.*, vol. 22, pp. 328–329, 1986.

[24] A. Alping, X. S. Wu, T. R. Hausken, and L. A. Coldren, "Highly efficient waveguide phase modulator for integrated optoelectronics," *Appl. Phys. Lett.*, vol. 48, pp. 1243–1245, 1986.

**Richard A. Soref** (S'58–M'63–SM'71) received the B.S.E.E. and M.S.E.E. degrees from the University of Wisconsin in 1958 and 1959, and the Ph.D. degree in electrical engineering from Stanford University, Stanford, CA, in 1963.

From 1963 to 1965, he worked in the optics and infrared group of M.I.T.'s Lincoln Laboratory, Cambridge, and in 1965, he joined the Technical Staff of the Sperry Research Center, Sudbury, MA, where he conducted research on a variety of topics including nonlinear optics, extrinsic Si infrared detectors, liquid crystal electrooptical devices, optical switching, and fiber-optic sensors. In November 1983, he joined the Rome Air Development Center, Hanscom, AFB, MA, as a Research Scientist in the Solid State Sciences Division. His current research interests include integrated optics and microwave applications of optics. He has authored and coauthored 70 journal articles and holds 14 patents.

Dr. Soref is a member of the American Physical Society, the Society of Photo-Optical Instrumentation Engineers, and the Optical Society of America. He served as Chairman of the Boston Chapter IEEE Group on Electron Devices in 1969. He is currently an Editorial Advisor of *Optical Engineering*.
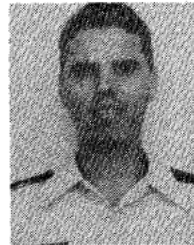


**Brian R. Bennett** was born in Overland Park, KS, in 1962. He received the B.S. and M.S. degrees, both in geophysics, from the Massachusetts Institute of Technology (M.I.T.), Cambridge, MA, in 1984 and 1985, respectively. As an undergraduate, he conducted research on the induced polarization of minerals. His M.S. thesis investigated the conductivity of the earth's crust and upper mantle using simultaneous measurements of electric and magnetic fields (the magentotelluric method).

He is currently serving in the U.S. Air Force in Bedford, MA, conducting research on low-temperature dielectric deposition and silicon integrated optics.

Mr. Bennett is a member of Sigma Xi, the American Physical Society, and the Materials Research Society.